

# Lecture I: Models for Nuclear Interactions

Morten Hjorth-Jensen<sup>1,2</sup>

<sup>1</sup>Department of Physics and Center of Mathematics for Applications  
University of Oslo, N-0316 Oslo

<sup>2</sup>Department of Physics and Astronomy, Michigan State University  
East Lansing, Michigan, USA

January 20, 2009

# Outline

- 1 Introduction and Motivation to the Lectures
- 2 Lecture I: Nuclear Interactions, from QCD to Effective Theories
  - Developing Models for the NN force
  - How to construct an Interaction: Partial Wave Analysis
  - Additional material: From QCD to Effective Field Theories

# Why CENS and what is it?

- AIM: To provide you with computational tools for nuclear structure analyses. Useful both for data analysis (finalizing articles, theses etc) as well as for writing proposals.
- CENS is a graphical user interface (GUI) written in Python which coordinates:
  - 1 Many programs in Fortran 90/95 for computing effective two-body interactions starting with free nucleon-nucleon interactions (proton-neutron formalism). Parallel codes available upon demand.
  - 2 A shell-model code and a transition code. Source code in C/C++ (portable to all systems) which allows you to address systems up to  $10^9$  basic states. Parallel codes for larger systems available upon demand.

# Why CENS and what is it?

- Weblink with codes and lectures:(<http://www.fys.uio.no/compphys/cp/software.html>) plus textbook to come (2009, with David Dean).
- First Release of GUI ([cens.tar.gz](http://cens.tar.gz)): september 2008.
- Understand how nuclear spectra evolve from the underlying nuclear interactions. Many types of effective interactions.
- Critical assessment of the methods, pros and cons and their limitations.

## Additions to come and further stuff

- 1 CENS-alpha version works for Linux/Unix and MAC. Windows version to come soon (end spring 2009).
- 2 Add possibility to do Coupled-Cluster calculations (end 2009)
- 3 Include three-body interaction and effective interaction diagrams (end 2009)
- 4 Add code to perform shell-model calculations with and without three-body interactions (end 2009)

# An alternative way to use the GUI

- 1 For large calculations the GUI is not very practical.
- 2 Use the GUI to generate the input files to the effective interaction calculation and the shell-model calculations.
- 3 Then run the shell-model or effective interaction codes on your local computing node(s).
- 4 **The GUI is then an easy to use tool to generate input files.**
- 5 This is the most likely usage of the GUI at the end.

# ORNL-OSLO Many-Body project, Code Developers

## ORNL

David Dean, Gaute Hagen, Thomas Papenbrock

## Oslo

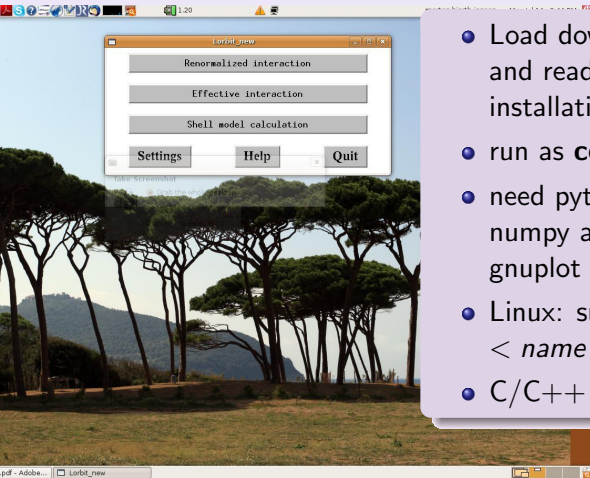
Elise Bergli, Torgeir Engeland, Morten Hjorth-Jensen, Gustav Jansen, Maxim Kartamychev, Simen Kvaal, Johannes Rekkedal

Lecture Plan, see also the link <http://www.fys.uio.no/compphys/cp/software.html>

- 1 Monday: Nuclear interactions, models and calculational schemes, from one-boson exchange models to effective field theories, file lecture1.pdf.
- 2 Tuesday: Methods for renormalizing the nucleon-nucleon interaction, Similarity transformation methods and link to many-body methods, file lecture2.pdf.
- 3 Wednesday: Many-body methods, we start with Hartree-Fock theory, large scale diagonalization methods (full configuration interaction or shell-model), many-body perturbation theory and coupled-cluster theory, file lecture3.pdf
- 4 Thursday: Applications of many-body methods and further properties of the different methods, file lecture4.pdf
- 5 Friday: From stable nuclei to weakly bound nuclei; choice of basis and many-body approaches. Possibly also how to link ab initio methods with density functional theory. File lecture5.pdf.



# CENS, with everything installed



- Load down the cens.tar.gz package and read the README file with installation prescriptions
- run as **cens**
- need python 2.4 (now python2.5), numpy and Pmw, Tkinter and gnuplot packages
- Linux: `sudo apt-get install < name - of - package >`
- C/C++ and Fortran 95 compilers

# Nuclear Many-Body Methods

- 1 Shell-model and No-core shell-model calculations; Large-scale diagonalization.
- 2 Perturbative many-body methods.
- 3 Coupled cluster theory
- 4 Extension to weakly bound systems. Complex scaling and complex shell model, Gamow shell model.
- 5 DFT and how to link it with ab initio methods
- 6 Density matrix renormalization group.
- 7 Variational, Diffusion and Path integral Monte Carlo methods.
- 8 Green's function theory, Unitary operator method....

# From Yukawa to Lattice QCD and Effective Field Theory

## 1930's

Chadwick (1932) discovers the neutron and Heisenberg (1932) proposes the first Phenomenology (Isospin). Yukawa (1935) and his Meson Hypothesis

## 1940's

Discovery of the pion in cosmic ray (1947) and in the Berkeley Cyclotron Lab (1948). Nobelprize awarded to Yukawa (1949). Rabi (1948) measures quadrupole moment of the deuteron.

## 1950's

Taketani, Nakamura, Sasaki (1951): 3 ranges. One-Pion-Exchange (OPE): o.k.  
Multi-pion exchanges: Problems! Taketani, Machida, Onuma (1952); "Pion Theories"  
Brueckner, Watson (1953).

# From Yukawa to Lattice QCD and Effective Field Theory

## 1960's

Many pions = multi-pion resonances:  $\sigma(600)$ ,  $\rho(770)$ ,  $\omega(782)$   
etc. One-Boson-Exchange Model. Refined Meson Theories

## 1970's

Sophisticated models for two-pion exchange: Paris Potential (Lacombe et al., Phys. Rev. C **21**, 861 (1980)) Bonn potential (Machleidt et al., Phys. Rep. **149**, 1 (1987))

## 1980's

Quark cluster models. Begin of effective field theory studies.

# From Yukawa to Lattice QCD and Effective Field Theory

## 1990's

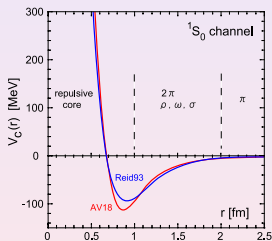
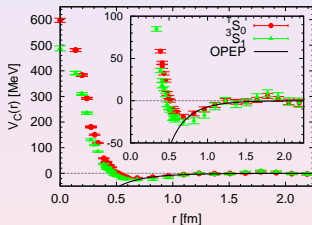
1993-2001: High-precision NN potentials: Nijmegen I, II, '93, Reid93 (Stoks et al. 1994), Argonne V18 (Wiringa et al, 1995), CD-Bonn (Machleidt et al. 1996 and 2001. Advances in effective field theory: Weinberg (1990); Ordonez, Ray, van Kolck and many more.

## 3rd Millenium

Another "pion theory"; but now right: constrained by chiral symmetry. Three-body and higher-body forces appear naturally at a given order of the chiral expansion.

## 2006

Nucleon-nucleon interaction from Lattice QCD, final confirmation of meson hypothesis of Yukawa?

Lattice QCD, Ishii *et al*, PRL 2007

The nucleon-nucleon interaction, Phenomenology vs Lattice calculations.

# Features of the Nucleon-Nucleon (NN) Force

The aim is to give you an overview over central features of the nucleon-nucleon interaction and how it is constructed, both technical and theoretical approaches.

- 1 The existence of the deuteron with  $J^\pi = 1^+$  indicates that the force between protons and neutrons is attractive at least for the  ${}^3S_1$  partial wave. Interference between Coulomb and nuclear scattering for the proton-proton partial wave  ${}^1S_0$  shows that the NN force is attractive at least for the  ${}^1S_0$  partial wave.
- 2 It has a short range and strong intermediate attraction.
- 3 Spin dependent, scattering lengths for triplet and singlet states are different,
- 4 Spin-orbit force. Observation of large polarizations of scattered nucleons perpendicular to the plane of scattering.

# Features of the Nucleon-Nucleon (NN) Force, continued

- 1 Hard core. The  $s$ -wave phase shift becomes negative at  $\approx 250$  MeV implying that the singlet  $S$  has a hard core with range  $0.4 - 0.5$  fm.
- 2 Charge independence (almost). Two nucleons in a given two-body state always (almost) experience the same force. Modern interactions break charge and isospin symmetry lightly. That means that the  $pp$ , neutron-neutron and  $pn$  parts of the interaction will be different for the same quantum numbers.
- 3 Non-central. There is a tensor force. First indications from the quadrupole moment of the deuteron pointing to an admixture in the ground state of both  $l = 2$  ( ${}^3D_1$ ) and  $l = 0$  ( ${}^3S_1$ ) orbital momenta.



# Short Range Evidence

Comparison of the binding energies of  ${}^2\text{H}$  (deuteron),  ${}^3\text{H}$  (triton),  ${}^4\text{He}$  (alpha - particle) show that the nuclear force is of finite range (1 – 2 fm) and very strong within that range. For nuclei with  $A > 4$ , the energy saturates: Volume and binding energies of nuclei are proportional to the mass number  $A$ .

Nuclei are also bound. The average distance between nucleons in nuclei is about 2 fm which must roughly correspond to the range of the attractive part.

# Charge Dependence

- After correcting for the electromagnetic interaction, the forces between nucleons (pp, nn, or np) in the same state are almost the same.
- "Almost the same": Charge-independence is slightly broken.
- Equality between the pp and nn forces: Charge symmetry.
- Equality between pp/nn force and np force: Charge independence.
- Better notation: Isospin symmetry, invariance under rotations in isospin

# Charge Dependence, $^1S_0$ Scattering Lengths

Charge-symmetry breaking (CSB), after electromagnetic effects have been removed:

- $a_{pp} = -17.3 \pm 0.4\text{fm}$
- $a_{nn} = -18.8 \pm 0.5\text{fm}$ . Note however discrepancy from  $nd$  breakup reactions resulting in  $a_{nn} = -18.72 \pm 0.13 \pm 0.65\text{fm}$  and  $\pi^- + d \rightarrow \gamma + 2n$  reactions giving  $a_{nn} = -18.93 \pm 0.27 \pm 0.3\text{fm}$ .

Charge-independence breaking (CIB)

- $a_{pn} = -23.74 \pm 0.02\text{fm}$

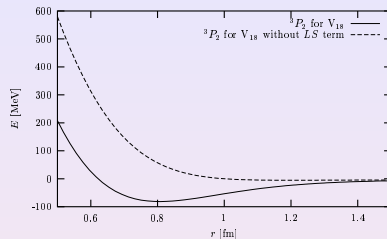
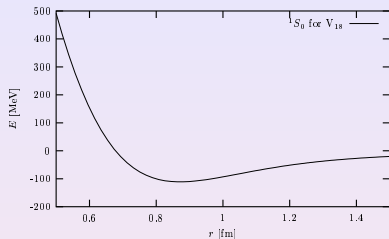
# Symmetries of the Nucleon-Nucleon (NN) Force

- 1 Translation invariance
- 2 Galilean invariance
- 3 Rotation invariance
- 4 Space reflection invariance
- 5 Time reversal invariance
- 6 Invariance under the interchange of particle 1 and 2
- 7 Almost isospin symmetry

A general two-body non-relativistic model under these symmetries was given by Okubo and Marshak, *Ann. Phys. (NY)* **4**, 166 (1958).

## CENS options

- 1 Charge symmetry breaking (CSB): available for N3LO and CD-Bonn interactions. All Argonne models include CSB.
- 2 Isospin symmetry breaking (ISB): available for N3LO and CD-Bonn interactions. All Argonne models include ISB.
- 3 Coulomb: Argonne includes Coulomb by default. All other interaction models can or cannot include the Coulomb interaction.







$$V(\mathbf{r}) = \left\{ C_c + C_\sigma \boldsymbol{\sigma}_1 \cdot \boldsymbol{\sigma}_2 + C_T \left( 1 + \frac{3}{m_\alpha r} + \frac{3}{(m_\alpha r)^2} \right) S_{12}(\hat{r}) \right. \\ \left. + C_{SL} \left( \frac{1}{m_\alpha r} + \frac{1}{(m_\alpha r)^2} \right) \mathbf{L} \cdot \mathbf{S} \right\} \frac{e^{-m_\alpha r}}{m_\alpha r}$$

How do we derive such terms?

# References for Various Phenomenological Interactions

Potentials which are based upon the standard non-relativistic operator structure are called "Phenomenological Potentials" Some historically important examples are

-  Gammel-Thaler potential ( Phys. Rev. **107**, 291, 1339 (1957) and the Hamada-Johnston potential, Nucl. Phys. **34**, 382 (1962)), bot with a hard core. core.
-  Reid potential (Ann. Phys. (N.Y.) **50**, 411 (1968)), soft core.
-  Argonne  $V_{14}$  potential (Wiringa et al., Phys. Rev. C **29**, 1207 (1984)) with 14 operators and the Argonne  $V_{18}$  potential (Wiringa et al., Phys. Rev. C **51**, 38 (1995)), uses 18 operators
-  A good reference: R. Machleidt, Adv. Nucl. Phys **19**, 189 (1989).

# Effective Degrees of Freedom

Since quantum chromodynamics (QCD) is commonly accepted as the theory of the strong interaction, the NN interaction  $V$  is completely determined by the underlying quark-quark dynamics in QCD. However, due to the non-perturbative character of QCD at low energies, one is still far from quantitative understanding of the NN interaction from the QCD point of view. Although there is no unique prescription for how to construct a free NN interaction, a description of the NN interaction in terms of various meson exchanges is presently the most quantitative representation of the NN interaction in the energy regime of low and medium energy nuclear physics, viz energies below 1 GeV.



# Effective Degrees of Freedom, History

- 1 From 1950 till approximately 2000: One-Boson-Exchange (OBE) models dominate
- 2 Now: models based on chiral perturbation theory.

## Dramatis Personae

Baryons	Mass (MeV)	Mesons	Mass (MeV)
$p, n$	938.926	$\pi$	138.03
$\Lambda$	1116.0	$\eta$	548.8
$\Sigma$	1197.3	$\sigma$	$\approx 550.0$
$\Delta$	1232.0	$\rho$	770
		$\omega$	782.6
		$\delta$	983.0
		$K$	495.8
		$K^*$	895.0

# Lagrangians

To describe the interaction between the various baryons and mesons of the previous table we choose the following phenomenological lagrangians for spin 1/2 baryons

$$\mathcal{L}_{ps} = g^{ps} \bar{\Psi} \gamma^5 \Psi \phi^{(ps)},$$

$$\mathcal{L}_s = g^s \bar{\Psi} \Psi \phi^{(s)},$$

and

$$\mathcal{L}_v = g^v \bar{\Psi} \gamma_\mu \Psi \phi_\mu^{(v)} + g^t \bar{\Psi} \sigma^{\mu\nu} \Psi \left( \partial_\mu \phi_\nu^{(v)} - \partial_\nu \phi_\mu^{(v)} \right),$$

for pseudoscalar (ps), scalar (s) and vector (v) coupling, respectively. The factors  $g^v$  and  $g^t$  are the vector and tensor coupling constants, respectively.

# Lagrangians, contn.

Similarly the factor  $g^s$  is the phenomenological coupling coefficient for scalar mesons while  $g^{ps}$  is the corresponding coupling constant for pseudoscalar meson exchanges. These coupling constants may be constrained by e.g. the nucleon-nucleon scattering data. In the above equations, we have defined  $\Psi$  to be the baryon field for spin 1/2 baryons, while  $\phi^{(ps)}$ ,  $\phi^{(s)}$  and  $\phi^{(v)}$  are the corresponding meson fields for pseudoscalar, scalar and vector mesons, respectively.

Note that the above equations are for isoscalar mesons, however, for isovector mesons, the fields  $\phi$  trivially modify to  $\tau\phi$  with  $\tau$  the familiar isospinor Pauli matrices.

# Spinors for Protons and Neutrons

For spin 1/2 baryons, the fields  $\Psi$  are expanded in terms of the Dirac spinors (positive energy solution shown here with  $\bar{u}u = 1$ )

$$u(k\sigma) = \sqrt{\frac{E(k) + m}{2m}} \begin{pmatrix} \chi \\ \frac{\boldsymbol{\sigma}\mathbf{k}}{E(k)+m}\chi \end{pmatrix},$$

with  $\chi$  the familiar Pauli spinor and  $E(k) = \sqrt{m^2 + |\mathbf{k}|^2}$ . The positive energy part of the field  $\Psi$  reads

$$\Psi(x) = \frac{1}{(2\pi)^{3/2}} \sum_{\mathbf{k}\sigma} u(k\sigma) e^{-ikx} a_{\mathbf{k}\sigma},$$

with  $a$  being a fermion annihilation operator.

# The Classical Expression

Expanding the free Dirac spinors in terms of  $1/m$  ( $m$  is here the mass of the relevant baryon) results, to lowest order, in the familiar non-relativistic expressions for baryon-baryon potentials. The configuration space version of the interaction can be approximated as

$$V(\mathbf{r}) = \left\{ C_C^0 + C_C^1 + C_\sigma \boldsymbol{\sigma}_1 \cdot \boldsymbol{\sigma}_2 + C_T \left( 1 + \frac{3}{m_\alpha r} + \frac{3}{(m_\alpha r)^2} \right) S_{12}(\hat{r}) + C_{SL} \left( \frac{1}{m_\alpha r} + \frac{1}{(m_\alpha r)^2} \right) \mathbf{L} \cdot \mathbf{S} \right\} \frac{e^{-m_\alpha r}}{m_\alpha r},$$

where  $m_\alpha$  is the mass of the relevant meson and  $S_{12}$  is the familiar tensor term.

# OBE for Scalar Mesons

Employing the above lagrangians, it is then possible to construct a one-boson-exchange potential model. Typically, a contribution  $V_s^{OBE}$  arising from the exchange of a scalar meson between two spin 1/2 baryons with equal masses is given by

$$\langle p'_1 p'_2 | V_s^{OBE} | p_1 p_2 \rangle = g_s^2 \frac{\bar{u}(p'_1) \bar{u}(p'_2) u(p_1) u(p_2)}{(p'_1 + p'_2 - p_1 - p_2)^2 - m_s^2},$$

where  $m_s$  is the mass of the exchanged scalar meson. What does it look like in coordinate space and what about pion exchange and the spin-orbit force?

# OBE for Pion Exchange

We derive now the non-relativistic one-pion exchange interaction. Here  $p_1$ ,  $p'_1$ ,  $p_2$ ,  $p'_2$  and  $k = p_1 - p'_1$  denote four-momenta. The vertices are given by the pseudovector Lagrangian

$$\mathcal{L}_{pv} = \frac{f_\pi}{m_\pi} \bar{\psi} \gamma_5 \gamma_\mu \psi \partial^\mu \phi_\pi.$$

From the Feynman diagram rules we can write the two-body interaction as

$$V^{pv} = \frac{f_\pi^2}{m_\pi^2} \frac{\bar{u}(p'_1) \gamma_5 \gamma_\mu (p_1 - p'_1)^\mu u(p_1) \bar{u}(p'_2) \gamma_5 \gamma_\nu (p_2 - p'_2)^\nu u(p_2)}{(p_1 - p'_1)^2 - m_\pi^2}.$$



# OBE for Pion Exchange

The factors  $p_1 - p'_1 = p'_2 - p_2$  are both the four-momentum of the exchanged meson and come from the derivative of the meson field in the interaction Lagrangian. The Dirac spinors obey

$$\begin{aligned}\gamma_\mu p^\mu u(p) &= mu(p) \\ \bar{u}(p)\gamma_\mu p^\mu &= m\bar{u}(p).\end{aligned}$$

Using these relations, together with  $\{\gamma_5, \gamma_\mu\} = 0$ , we find

$$\begin{aligned}\bar{u}(p'_1)\gamma_5\gamma_\mu(p_1 - p'_1)^\mu u(p_1) &= m\bar{u}(p'_1)\gamma_5 u(p_1) + \bar{u}(p'_1)\gamma_\mu p_1'^\mu \gamma_5 u(p_1) \\ &= 2m\bar{u}(p'_1)\gamma_5 u(p_1)\end{aligned}$$

and

$$\bar{u}(p'_2)\gamma_5\gamma_\mu(p'_2 - p_2)^\mu = -2m\bar{u}(p'_2)\gamma_5 u(p_2).$$

## OBE for Pion Exchange

We get

$$V^{pv} = -\frac{f_\pi^2}{m_\pi^2} 4m^2 \frac{\bar{u}(p'_1)\gamma_5 u(p_1)\bar{u}(p'_2)\gamma_5 u(p_2)}{(p_1 - p'_1)^2 - m_\pi^2}.$$

By inserting expressions for the Dirac spinors, we find

$$\begin{aligned} \bar{u}(p'_1)\gamma_5 u(p_1) &= \sqrt{\frac{(E'_1 + m)(E_1 + m)}{4m^2}} \begin{pmatrix} \chi^\dagger & -\frac{\sigma_1 \cdot \mathbf{p}_1}{E'_1 + m} \chi^\dagger \end{pmatrix} \begin{pmatrix} 0 & 1 \\ 1 & 0 \end{pmatrix} \\ &\quad \times \begin{pmatrix} \chi \\ \frac{\sigma_1 \cdot \mathbf{p}_1}{E_1 + m} \chi \end{pmatrix} \\ &= \sqrt{\frac{(E'_1 + m)(E_1 + m)}{4m^2}} \begin{pmatrix} \sigma_1 \cdot \mathbf{p}_1 & -\sigma_1 \cdot \mathbf{p}'_1 \\ E_1 + m & E'_1 + m \end{pmatrix} \end{aligned}$$

# OBE for Pion Exchange

Similarly

$$\bar{u}(p'_2)\gamma_5 u(p_1) = \sqrt{\frac{(E'_2 + m)(E_2 + m)}{4m^2}} \left( \frac{\sigma_2 \cdot \mathbf{p}_2}{E_2 + m} - \frac{\sigma_2 \cdot \mathbf{p}'_2}{E'_2 + m} \right).$$

In the CM system we have  $\mathbf{p}_2 = -\mathbf{p}_1$ ,  $\mathbf{p}'_2 = -\mathbf{p}'_1$  and so  $E_2 = E_1$ ,  $E'_2 = E'_1$ . We can then write down the relativistic contribution to the NN potential in the CM system:

$$V^{p\nu} = -\frac{f_\pi^2}{m_\pi^2} 4m^2 \frac{1}{(p_1 - p'_1)^2 - m_\pi^2} \frac{(E_1 + m)(E'_1 + m)}{4m^2} \\ \times \left( \frac{\sigma_1 \cdot \mathbf{p}_1}{E_1 + m} - \frac{\sigma_1 \cdot \mathbf{p}'_1}{E'_1 + m} \right) \left( \frac{\sigma_2 \cdot \mathbf{p}_1}{E_1 + m} - \frac{\sigma_2 \cdot \mathbf{p}'_1}{E'_1 + m} \right).$$

# OBE for Pion Exchange

In the non-relativistic limit we have to lowest order

$$E_1 = \sqrt{\mathbf{p}_1^2 + m^2} \approx m \approx E'_1$$

and then  $(p_1 - p'_1)^2 = -\mathbf{k}^2$ , so we get for the contribution to the NN potential

$$\begin{aligned} V^{pv} &= -\frac{f_\pi^2}{m_\pi^2} 4m^2 \frac{1}{\mathbf{k}^2 + m^2} \frac{2m \cdot 2m}{4m^2} \frac{\sigma_1}{2m} \cdot (\mathbf{p}_1 - \mathbf{p}'_1) \frac{\sigma_2}{2m} \cdot (\mathbf{p}_1 - \mathbf{p}'_1) \\ &= -\frac{f_\pi^2}{m_\pi^2} \frac{(\sigma_1 \cdot \mathbf{k})(\sigma_2 \cdot \mathbf{k})}{\mathbf{k}^2 + m_\pi^2}. \end{aligned}$$

We have omitted exchange terms and isospin  $\boldsymbol{\tau}_1 \cdot \boldsymbol{\tau}_2$ .

# OBE for Pion Exchange, from $k$ -space to $r$ -space

We have

$$V^{pv}(k) = -\frac{f_\pi^2}{m_\pi^2} \frac{(\sigma_1 \cdot \mathbf{k})(\sigma_2 \cdot \mathbf{k})}{\mathbf{k}^2 + m_\pi^2} \boldsymbol{\tau}_1 \cdot \boldsymbol{\tau}_2.$$

In coordinate space we have

$$V^{pv}(r) = \int \frac{d^3k}{(2\pi)^3} e^{i\mathbf{k}\mathbf{r}} V^{pv}(k)$$

resulting in

$$V^{pv}(r) = \frac{f_\pi^2}{m_\pi^2} \boldsymbol{\tau}_1 \cdot \boldsymbol{\tau}_2 \sigma_1 \cdot \nabla \sigma_2 \cdot \nabla \int \frac{d^3k}{(2\pi)^3} e^{i\mathbf{k}\mathbf{r}} \frac{1}{\mathbf{k}^2 + m_\pi^2}.$$

We obtain

$$V^{pv}(r) = \frac{f_\pi^2}{m_\pi^2} \boldsymbol{\tau}_1 \cdot \boldsymbol{\tau}_2 \sigma_1 \cdot \nabla \sigma_2 \cdot \nabla \frac{e^{-m_\pi r}}{r}.$$

# OBE for Pion Exchange, really the last Step (I promise)

Carrying out the differentiation of

$$V^{PV}(r) = \frac{f_\pi^2}{m_\pi^2} \boldsymbol{\tau}_1 \cdot \boldsymbol{\tau}_2 \boldsymbol{\sigma}_1 \cdot \nabla \boldsymbol{\sigma}_2 \cdot \nabla \frac{e^{-m_\pi r}}{r}.$$

we arrive at the famous one-pion exchange potential with central and tensor parts

$$V(r) = \frac{f_\pi^2}{m_\pi^2} \boldsymbol{\tau}_1 \cdot \boldsymbol{\tau}_2 \left\{ \boldsymbol{\sigma}_1 \cdot \boldsymbol{\sigma}_2 + C_T \left( 1 + \frac{3}{m_\alpha r} + \frac{3}{(m_\alpha r)^2} \right) S_{12}(\hat{r}) \right\} \frac{e^{-m_\pi r}}{m_\pi r}.$$

For the full potential add the exchange part + isospin dependence as well.

## Other Mesons: Collecting Terms, $\sigma$

When we perform similar non-relativistic expansions for scalar and vector mesons we obtain for the  $\sigma$  meson

$$V^\sigma = g_{\sigma NN}^2 \frac{1}{\mathbf{k}^2 + m_\sigma^2} \left( -1 + \frac{\mathbf{q}^2}{2M_N^2} - \frac{\mathbf{k}^2}{8M_N^2} - \frac{\mathbf{L}\mathbf{S}}{2M_N^2} \right).$$

We note an attractive central force and spin-orbit force. This term has an intermediate range. We have defined  $1/2(p_1 + p_1') = \mathbf{q}$ .

## Other Mesons: Collecting Terms, $\omega$

We obtain for the  $\omega$  meson

$$V^\omega = g_{\omega NN}^2 \frac{1}{\mathbf{k}^2 + m_\omega^2} \left( 1 - 3 \frac{\mathbf{L}\mathbf{S}}{2M_N^2} \right).$$

We note a repulsive central force and attractive spin-orbit force.  
This term has short range.



## Other Mesons: Collecting Terms, $\rho$

Finally for the  $\rho$  meson

$$V^\rho = g_{\rho NN}^2 \frac{\mathbf{k}^2}{\mathbf{k}^2 + m_\rho^2} \left( -2\sigma_1\sigma_2 + S_{12}(\hat{k}) \right) \tau_1\tau_2.$$

We note a tensor force with sign opposite to that of the pion. This term has short range.

# CENS options

- 1 You can compute a pure one-pion exchange interaction, option OPEP
- 2 Or you can just study the role of the LS interaction
- 3 Or just the tensor force.

All these options are derived using the parameterizations of the Argonne  $V8$  interaction model.

## Brief summary from Monday's lecture

- 1 Can use a one-boson exchange picture to construct a nucleon-nucleon interaction a la QED
- 2 Non-relativistic approximation yields amongst other things a spin-orbit force which is much stronger than in atoms.
- 3 At large intermediate distances pion exchange dominates while pion resonances (other mesons) dominate at intermediate and short range
- 4 Potentials are parameterized to fit selected two-nucleon data, binding energies and scattering phase shifts.
- 5 Nowadays, chiral perturbation theory gives an effective theory that allows a systematic expansion in terms of controllable parameters. Good basis for many-body physics

# Mathematical Intermezzo, two-body Schrödinger in $k$ -space

The Schrödinger equation in abstract vector representation is

$$(T + V) |\psi_n\rangle = E_n |\psi_n\rangle \quad (1)$$

Here  $T$  is the kinetic energy operator and  $V$  is the potential operator. The eigenstates form a complete orthonormal set according to

$$\mathbf{1} = \sum_n |\psi_n\rangle \langle \psi_n|, \quad \langle \psi_n | \psi_{n'} \rangle = \delta_{n,n'}$$

# Mathematical Intermezzo, two-body Schrödinger in $k$ -space

The most commonly used representations of equation 1 are the coordinate and the momentum space representations. They define the completeness relations

$$\mathbf{1} = \int d\mathbf{r} |\mathbf{r}\rangle\langle\mathbf{r}|, \quad \langle\mathbf{r}|\mathbf{r}'\rangle = \delta(\mathbf{r} - \mathbf{r}') \quad (2)$$

$$\mathbf{1} = \int d\mathbf{k} |\mathbf{k}\rangle\langle\mathbf{k}|, \quad \langle\mathbf{k}|\mathbf{k}'\rangle = \delta(\mathbf{k} - \mathbf{k}') \quad (3)$$

Here the basis states in both  $\mathbf{r}$ - and  $\mathbf{k}$ -space are dirac-delta function normalized. From this it follows that the plane-wave states are given by,

$$\langle\mathbf{r}|\mathbf{k}\rangle = \left(\frac{1}{2\pi}\right)^{3/2} \exp(i\mathbf{k} \cdot \mathbf{r}) \quad (4)$$

which is a transformation function defining the mapping from the abstract  $|\mathbf{k}\rangle$  to the abstract  $|\mathbf{r}\rangle$  space.

# Mathematical Intermezzo, two-body Schrödinger in $k$ -space

That the  $\mathbf{r}$ -space basis states are delta-function normalized follows from

$$\delta(\mathbf{r} - \mathbf{r}') = \langle \mathbf{r} | \mathbf{r}' \rangle = \langle \mathbf{r} | \mathbf{1} | \mathbf{r}' \rangle = \int d\mathbf{k} \langle \mathbf{r} | \mathbf{k} \rangle \langle \mathbf{k} | \mathbf{r}' \rangle = \left( \frac{1}{2\pi} \right)^3 \int d\mathbf{k} e^{i\mathbf{k}(\mathbf{r} - \mathbf{r}')} \quad (5)$$

and the same for the momentum space basis states,

$$\delta(\mathbf{k} - \mathbf{k}') = \langle \mathbf{k} | \mathbf{k}' \rangle = \langle \mathbf{k} | \mathbf{1} | \mathbf{k}' \rangle = \int d\mathbf{r} \langle \mathbf{k} | \mathbf{r} \rangle \langle \mathbf{r} | \mathbf{k}' \rangle = \left( \frac{1}{2\pi} \right)^3 \int d\mathbf{r} e^{i\mathbf{r}(\mathbf{k} - \mathbf{k}')} \quad (6)$$

# Mathematical Intermezzo, two-body Schrödinger in $k$ -space

Projecting equation 1 on momentum states the momentum space Schrödinger equation is obtained,

$$\frac{\hbar^2}{2\mu} k^2 \psi_n(\mathbf{k}) + \int d\mathbf{k}' V(\mathbf{k}, \mathbf{k}') \psi_n(\mathbf{k}') = E_n \psi_n(\mathbf{k}) \quad (7)$$

Here the notation  $\psi_n(\mathbf{k}) = \langle \mathbf{k} | \psi_n \rangle$  and  $\langle \mathbf{k} | V | \mathbf{k}' \rangle = V(\mathbf{k}, \mathbf{k}')$  has been introduced. The potential in momentum space is given by a double Fourier-transform of the potential in coordinate space, i.e.

$$V(\mathbf{k}, \mathbf{k}') = \left( \frac{1}{2\pi} \right)^3 \int d\mathbf{r} \int d\mathbf{r}' e^{-i\mathbf{k}\mathbf{r}} V(\mathbf{r}, \mathbf{r}') e^{i\mathbf{k}'\mathbf{r}'} \quad (8)$$

# Mathematical Intermezzo, two-body Schrödinger in $k$ -space

Here it is assumed that the potential interaction does not contain any spin dependence. Instead of a differential equation in coordinate space, the Schrödinger equation becomes an integral equation in momentum space. This has many tractable features. Firstly, most realistic nucleon-nucleon interactions derived from field-theory are given explicitly in momentum space. Secondly, the boundary conditions imposed on the differential equation in coordinate space are automatically built into the integral equation. And last, but not least, integral equations are easy to numerically implement, and convergence is obtained by just increasing the number of integration points. Instead of solving the three-dimensional integral equation given in equation (7), an infinite set of 1-dimensional equations can be obtained via a partial wave expansion.



# Mathematical Intermezzo, two-body Schrödinger in $k$ -space

The wave function  $\psi_n(\mathbf{k})$  can be expanded in a complete set of spherical harmonics, i.e.

$$\psi_n(\mathbf{k}) = \sum_{lm} \psi_{nlm}(k) Y_{lm}(\hat{k}), \quad \psi_{nlm}(k) = \int d\hat{k} Y_{lm}^*(\hat{k}) \psi_n(\mathbf{k}). \quad (9)$$

By inserting equation 9 in equation 7, and projecting from the left  $Y_{lm}(\hat{k})$ , the three-dimensional Schrödinger equation (7) is reduced to an infinite set of 1-dimensional angular momentum coupled integral equations,

$$\left( \frac{\hbar^2}{2\mu} k^2 - E_{nlm} \right) \psi_{nlm}(k) = - \sum_{l'm'} \int_0^\infty dk' k'^2 V_{lm,l'm'}(k, k') \psi_{nl'm'}(k') \quad (10)$$

where the angular momentum projected potential takes the form,

$$V_{lm,l'm'}(k, k') = \int d\hat{k} \int d\hat{k}' Y_{lm}^*(\hat{k}) V(\mathbf{k}, \mathbf{k}') Y_{l'm'}(\hat{k}') \quad (11)$$

# Mathematical Intermezzo, two-body Schrödinger in $k$ -space

Often the potential is given in position space, so it is convenient to establish the connection between  $V_{lm,l'm'}(k, k')$  and  $V_{lm,l'm'}(r, r')$ . Inserting position space completeness in equation (11) gives

$$\begin{aligned} V_{lm,l'm'}(k, k') &= \int d\mathbf{r} \int d\mathbf{r}' \int d\hat{k} \int d\hat{k}' Y_{lm}^*(\hat{k}) \langle \mathbf{k} | \mathbf{r} \rangle \langle \mathbf{r} | V | \mathbf{r}' \rangle \langle \mathbf{r}' | \mathbf{k}' \rangle Y_{lm}(\hat{k}') \\ &= \int d\mathbf{r} \int d\mathbf{r}' \left\{ \int d\hat{k} Y_{lm}^*(\hat{k}) \langle \mathbf{k} | \mathbf{r} \rangle \right\} \\ &\quad \times \langle \mathbf{r} | V | \mathbf{r}' \rangle \left\{ \int d\hat{k}' Y_{lm}(\hat{k}') \langle \mathbf{r}' | \mathbf{k}' \rangle \right\} \end{aligned} \quad (12)$$

# Mathematical Intermezzo, two-body Schrödinger in $k$ -space

Since the plane waves depend only on the absolute values of position and momentum,  $|\mathbf{k}|$ ,  $|\mathbf{r}|$ , and the angle between them,  $\theta_{kr}$ , they may be expanded in terms of bipolar harmonics of zero rank, i.e.

$$e^{i\mathbf{k}\cdot\mathbf{r}} = 4\pi \sum_{l=0}^{\infty} i^l j_l(kr) \left( Y_l(\hat{\mathbf{k}}) \cdot Y_l(\hat{\mathbf{r}}) \right) = \sum_{l=0}^{\infty} (2l+1) i^l j_l(kr) P_l(\cos \theta_{kr}) \quad (13)$$

where the addition theorem for spherical harmonics has been used in order to write the expansion in terms of Legendre polynomials. The spherical Bessel functions,  $j_l(z)$ , are given in terms of Bessel functions of the first kind with half integer orders,

$$j_l(z) = \sqrt{\frac{\pi}{2z}} J_{l+1/2}(z).$$

# Mathematical Intermezzo, two-body Schrödinger in $k$ -space

Inserting the plane-wave expansion into the brackets of equation (12) yields,

$$\int d\hat{k} Y_{lm}^*(\hat{k}) \langle \mathbf{k} | \mathbf{r} \rangle = \left( \frac{1}{2\pi} \right)^{3/2} 4\pi i^{-l} j_l(kr) Y_{lm}^*(\hat{r}),$$
$$\int d\hat{k}' Y_{lm}(\hat{k}') \langle \mathbf{r}' | \mathbf{k}' \rangle = \left( \frac{1}{2\pi} \right)^{3/2} 4\pi i^{l'} j_{l'}(k'r') Y_{l'm'}(\hat{r}').$$

# Mathematical Intermezzo, two-body Schrödinger in $k$ -space

The connection between the momentum- and position space angular momentum projected potentials are then given,

$$V_{lm,l'm'}(k, k') = \frac{2}{\pi} i^{l'-l} \int_0^\infty dr r^2 \int_0^\infty dr' r'^2 j_l(kr) V_{lm,l'm'}(r, r') j_{l'}(k'r') \quad (14)$$

which is known as a double Fourier-Bessel transform. The position space angular momentum projected potential is given by

$$V_{lm,l'm'}(r, r') = \int d\hat{r} \int d\hat{r}' Y_{lm}^*(\hat{r}) V(\mathbf{r}, \mathbf{r}') Y_{l'm'}(\hat{r}'). \quad (15)$$

# Mathematical Intermezzo, two-body Schrödinger in $k$ -space

No assumptions of locality/non-locality and deformation of the interaction has so far been made, and the result in equation (14) is general. In position space the Schrödinger equation takes form of an integro-differential equation in case of a non-local interaction, in momentum space the Schrödinger equation is an ordinary integral equation of the Fredholm type, see equation (10). This is a further advantage of the momentum space approach as compared to the standard position space approach. If we assume that the interaction is of local character, i.e.

$$\langle \mathbf{r} | V | \mathbf{r}' \rangle = V(\mathbf{r}) \delta(\mathbf{r} - \mathbf{r}') = V(\mathbf{r}) \frac{\delta(r - r')}{r^2} \delta(\cos \theta - \cos \theta') \delta(\varphi - \varphi'),$$

then equation (15) reduces to

$$V_{lm,l'm'}(r, r') = \frac{\delta(r - r')}{r^2} \int d\hat{r} Y_{lm}^*(\hat{r}) V(\mathbf{r}) Y_{l'm'}(\hat{r}), \quad (16)$$

# Mathematical Intermezzo, two-body Schrödinger in $k$ -space

and equation (14) reduces to

$$V_{lm,l'm'}(k, k') = \frac{2}{\pi} i^{l'-l} \int_0^\infty dr r^2 j_l(kr) V_{lm,l'm'}(r) j_{l'}(k'r) \quad (17)$$

where

$$V_{lm,l'm'}(r) = \int d\hat{r} Y_{lm}^*(\hat{r}) V(\mathbf{r}) Y_{l'm'}(\hat{r}), \quad (18)$$

# Mathematical Intermezzo, two-body Schrödinger in $k$ -space

In the case that the interaction is central,  $V(\mathbf{r}) = V(r)$ , then

$$V_{lm,l'm'}(r) = V(r) \int d\hat{r} Y_{lm}^*(\hat{r}) Y_{l'm'}(\hat{r}) = V(r) \delta_{l,l'} \delta_{m,m'}, \quad (19)$$

and

$$V_{lm,l'm'}(k, k') = \frac{2}{\pi} \int_0^\infty dr r^2 j_l(kr) V(r) j_{l'}(k'r) \delta_{l,l'} \delta_{m,m'} = V_l(k, k') \delta_{l,l'} \delta_{m,m'} \quad (20)$$

where the momentum space representation of the interaction finally reads,

$$V_l(k, k') = \frac{2}{\pi} \int_0^\infty dr r^2 j_l(kr) V(r) j_l(k'r). \quad (21)$$



# Mathematical Intermezzo, two-body Schrödinger in $k$ -space

For a local and spherical symmetric potential, the coupled momentum space Schrödinger equations given in equation (10) decouples in angular momentum, giving

$$\frac{\hbar^2}{2\mu} k^2 \psi_{nl}(k) + \int_0^\infty dk' k'^2 V_l(k, k') \psi_{nl}(k') = E_{nl} \psi_{nl}(k) \quad (22)$$

Where we have written  $\psi_{nl}(k) = \psi_{nlm}(k)$ , since the equation becomes independent of the projection  $m$  for spherical symmetric interactions. The momentum space wave functions  $\psi_{nl}(k)$  defines a complete orthogonal set of functions, which spans the space of functions with a positive finite Euclidean norm (also called  $l^2$ -norm),  $\sqrt{\langle \psi_n | \psi_n \rangle}$ , which is a Hilbert space. The corresponding normalized wave function in coordinate space is given by the Fourier-Bessel transform

$$\phi_{nl}(r) = \sqrt{\frac{2}{\pi}} \int dk k^2 j_l(kr) \psi_{nl}(k) \quad (23)$$

# Bethe-Salpeter Equation

In order to obtain the parameters which define an NN potential derived from OBE or chiral perturbation theory models, the Bethe-Salpeter equation is used as the starting point for most calculations. This equation serves to define a two-particle interaction  $\mathcal{T}$ , meant to reproduce properties like low-energy scattering data. The fully covariant Bethe-Salpeter equation reads (suppressing spin and isospin) in an arbitrary frame

$$\begin{aligned} \langle p'_1 p'_2 | \mathcal{T} | p_1 p_2 \rangle &= \langle p'_1 p'_2 | \mathcal{V} | p_1 p_2 \rangle \\ &+ \frac{i}{(2\pi)^4} \int d^4 k \langle p'_1 p'_2 | \mathcal{V} | P + k, P - k \rangle \\ &\times S_{(1)}(P + k) S_{(2)}(P - k) \langle P + k, P - k | \mathcal{T} | p_1 p_2 \rangle . \end{aligned}$$

# Bethe-Salpeter Equation, contn.

Here we have defined  $P$  to be *half* the total four-momentum, i.e.  $P = \frac{1}{2}(p_1 + p_2)$ , and  $k$  to be the relative four-momentum. The term  $S_{(i)}$  is the fermion propagator, which for e.g. positive energy spin 1/2 baryons reads

$$S_{(i)}(p) = (\not{p}_i - m_i + i\epsilon)^{-1},$$

with the subscript  $i$  referring to baryon  $i$ .

# Bethe-Salpeter Equation, contn.

In principle  $\mathcal{V}$  is supposed to represent all kinds of irreducible two-particle interactions, though it is commonly approximated by the lowest order two-particle diagram. With this prescription we obtain the familiar ladder approach to the Bethe-Salpeter equation, similar to the approach discussed in connection with the  $G$ -matrix. The schematic structure of the ladder equation is representative for both the scattering matrix and the reaction matrix  $G$ . It is a four-dimensional integral equation, which is rather tedious to solve numerically.

# Bethe-Salpeter Equation, contn.

It is therefore commonly replaced by a three-dimensional quasi-potential equation, where the time components of the four-momenta of the incoming and outgoing particles have been fixed by some adequate choice. Still in an arbitrary frame we get

$$\begin{aligned} \langle \mathbf{p}'_1 \mathbf{p}'_2 | T | \mathbf{p}_1 \mathbf{p}_2 \rangle &= \langle \mathbf{p}'_1 \mathbf{p}'_2 | V | \mathbf{p}_1 \mathbf{p}_2 \rangle \\ &+ \frac{1}{(2\pi)^3} \int d^3 k \langle \mathbf{p}'_1 \mathbf{p}'_2 | V | \mathbf{P} + \mathbf{k}, \mathbf{P} - \mathbf{k} \rangle \\ &g(\mathbf{k}, s) \langle \mathbf{P} + \mathbf{k}, \mathbf{P} - \mathbf{k} | T | \mathbf{p}_1 \mathbf{p}_2 \rangle. \end{aligned}$$

$V$  is now the so-called “quasi-potential”, with fixed time components of the in- and outgoing particle momenta. As such, it is no longer an independent quantity. A much favored choice is to fix  $p_1^0 = p_2^0 = \frac{1}{2}\sqrt{s}$ ,  $s = (p_1 + p_2)^2$ .

## Bethe-Salpeter Equation, contn.

This prescription puts the two particles symmetrically off-shell, and is used in connection with the Blankenbecler-Sugar equation. The latter is one possibility of several three-dimensional reductions of the Bethe-Salpeter equation. The quantity  $g$  is related to the baryon propagators  $S_{(1)}S_{(2)}$  through

$$g(\mathbf{k}, s) = -i \int dk_0 S_{(1)}(k) S_{(2)}(-k).$$

The Blankenbecler-Sugar choice for  $g$  is (assuming  $m_1 = m_2$  and spin 1/2 fermions)

$$g(\mathbf{k}, s) = \frac{m^2 \Lambda_{(1)}^+(\mathbf{k}) \Lambda_{(2)}^+(-\mathbf{k})}{E_k \left[ \frac{1}{4}s - E_k^2 + i\epsilon \right]}.$$

All NN potentials reproduce essentially the same set of low-energy NN scattering data ( $E_{lab} \leq 350$  MeV) and properties of the deuteron. These are referred to as the “on-shell” properties of an NN potential, since all potential models result in a roughly similar on-shell scattering matrix  $T$ . The crucial point is then the differing off-shell behavior of the NN potentials in nuclear structure studies. The Bethe-Salpeter equation reads in the center-of-mass system (omitting angular momentum, isospin, spin etc. assignments)

$$T(\mathbf{k}, \mathbf{k}') = V(\mathbf{k}, \mathbf{k}') + \int_0^\infty \frac{d^3q}{(2\pi)^3} V(\mathbf{k}, \mathbf{q}) \frac{M_N^2}{E_q} \frac{\Lambda_{(1)}^+(\mathbf{q}) \Lambda_{(2)}^+(-\mathbf{q})}{\mathbf{k}^2 - \mathbf{q}^2 + i\epsilon} T(\mathbf{q}, \mathbf{k}'),$$

where  $E_q = \sqrt{M_N^2 + \mathbf{q}^2}$ .

# Three-dimensional Reduction

For positive-energy spinors

$$T(\mathbf{k}, \mathbf{k}') = V(\mathbf{k}, \mathbf{k}') + \int_0^\infty \frac{d^3q}{(2\pi)^3} V(\mathbf{k}, \mathbf{q}) \frac{M_N^2}{E_q} \frac{1}{\mathbf{k}^2 - \mathbf{q}^2 + i\epsilon} T(\mathbf{q}, \mathbf{k}').$$

Using

$$\hat{T}(\mathbf{k}, \mathbf{k}') = \sqrt{\frac{M_N}{E_{k'}}} T(\mathbf{k}, \mathbf{k}') \sqrt{\frac{M_N}{E_k}},$$

and

$$\hat{V}(\mathbf{k}, \mathbf{k}') = \sqrt{\frac{M_N}{E_{k'}}} V(\mathbf{k}, \mathbf{k}') \sqrt{\frac{M_N}{E_k}},$$

gives

$$\hat{T}(\mathbf{k}, \mathbf{k}') = \hat{V}(\mathbf{k}, \mathbf{k}') + \int_0^\infty \frac{d^3q}{(2\pi)^3} \hat{V}(\mathbf{k}, \mathbf{q}) \frac{1}{\mathbf{k}^2 - \mathbf{q}^2 + i\epsilon} \hat{T}(\mathbf{q}, \mathbf{k}').$$



# First Solution Step

In terms of the relative and center-of-mass momenta  $\mathbf{k}$  and  $\mathbf{K}$ , the potential in momentum space is related to the nonlocal operator  $V(\mathbf{r}, \mathbf{r}')$  by

$$\langle \mathbf{k}' \mathbf{K}' | V | \mathbf{k} \mathbf{K} \rangle = \int d\mathbf{r} d\mathbf{r}' e^{-i\mathbf{k}'\mathbf{r}'} V(\mathbf{r}', \mathbf{r}) e^{i\mathbf{k}\mathbf{r}} \delta(\mathbf{K}, \mathbf{K}').$$

We will assume that the interaction is spherically symmetric. Can separate the radial part of the wave function from its angular dependence. The wave function of the relative motion is described in terms of plane waves as

$$e^{i\mathbf{k}\mathbf{r}} = \langle \mathbf{r} | \mathbf{k} \rangle = 4\pi \sum_{lm} i^l j_l(kr) Y_{lm}^*(\hat{\mathbf{k}}) Y_{lm}(\hat{\mathbf{r}}),$$

where  $j_l$  is a spherical Bessel function and  $Y_{lm}$  the spherical harmonic.

# Decomposing the NN Force

This partial wave basis is useful for defining the operator for the nucleon-nucleon interaction, which is symmetric with respect to rotations, parity and isospin transformations. These symmetries imply that the interaction is diagonal with respect to the quantum numbers of total angular momentum  $J$ , spin  $S$  and isospin  $T$ . Using the above plane wave expansion, and coupling to final  $J$ ,  $S$  and  $T$  we get

$$\begin{aligned} \langle \mathbf{k}' | V | \mathbf{k} \rangle &= (4\pi)^2 \sum_{STI'I'mJ} i^{l+l'} Y_{lm}^*(\hat{\mathbf{k}}) Y_{l'm'}(\hat{\mathbf{k}}') \\ &\times C_{m'M_S M}^{l'SJ} C_{mM_S M}^{lSJ} \langle k'I'STJM | V | kISTJM \rangle, \end{aligned}$$

where we have defined

$$\langle k'I'STJM | V | kISTJM \rangle = \int j_{l'}(k'r') \langle l'STJM | V(r', r) | lSTJM \rangle j_l(kr) r'^2$$

The general structure of the  $T$ -matrix is

$$T_{ll'}^{\alpha}(kk'K\omega) = V_{ll'}^{\alpha}(kk')$$

$$+ \frac{2}{\pi} \sum_{l''mM_S} \int_0^{\infty} d\mathbf{q} (C_{mM_S}^{l''S\mathcal{J}})^2 \frac{Y_{l''m}^*(\hat{\mathbf{q}}) Y_{l''m}(\hat{\mathbf{q}}) V_{ll''}^{\alpha}(kq) T_{l''l'}^{\alpha}(qk'K\omega)}{\omega - H_0},$$

The shorthand notation

$$T_{ll'}^{\alpha}(kk'K\omega) = \langle kKlL\mathcal{J}ST | T(\omega) | k'Kl'L\mathcal{J}ST \rangle,$$

denotes the  $T$ -matrix with momenta  $k$  and  $k'$  and orbital momenta  $l$  and  $l'$  of the relative motion, and  $K$  is the corresponding momentum of the center-of-mass motion. Further,  $L$ ,  $\mathcal{J}$ ,  $S$  and  $T$  are the orbital momentum of the center-of-mass motion, the total angular momentum, spin and isospin, respectively.

Using the orthogonality properties of the Clebsch-Gordan coefficients and the spherical harmonics, we obtain the well-known one-dimensional angle independent integral equation

$$T_{ll'}^{\alpha}(kk'K\omega) = V_{ll'}^{\alpha}(kk') + \frac{2}{\pi} \sum_{l''} \int_0^{\infty} dq q^2 \frac{V_{ll''}^{\alpha}(kq) T_{l''l'}^{\alpha}(qk'K\omega)}{\omega - H_0}.$$

Inserting the denominators for the Blankenbecler-Sugar of the full Bethe-Salpeter equation we arrive at

$$\hat{T}_{ll'}^{\alpha}(kk'K) = \hat{V}_{ll'}^{\alpha}(kk') + \frac{2}{\pi} \sum_{l''} \int_0^{\infty} dq q^2 \hat{V}_{ll''}^{\alpha}(kq) \frac{1}{k^2 - q^2 + i\epsilon} \hat{T}_{l''l'}^{\alpha}(qk'K).$$

Note that the OBE models, via the solution of the Bethe-Salpeter equation contain only a selected class of diagrams. However, there are also non-iterative diagrams which contribute to the nuclear force.

# CENS options

- 1 You can choose to omit or include particular partial waves under the **options** knob of the renormalization part. The variables refer to the minimum and maximum  $J$  in the relative coordinates.
- 2 Note that the Argonne model is parameterized with  $J \leq 4$ .
- 3 Data are scanty above  $J > 5$  and the other interaction models give therefore only theoretical predictions.
- 4 For the no-core, vlowk, v-krp and v-nrg options, beyond  $J > 6$  the Hamiltonian is given by kinetic energy only.

## CENS image

The screenshot displays the 'Renormalized Interaction' software interface. The main window shows two panels: 'Neutron orbits' and 'Proton orbits'. Each panel displays energy levels (e.g., 1h 9/2, 3s 1/2, 2d 3/2) and the number of particles (represented by green and red dots) occupying those levels. The 'Options' dialog box is open, showing settings for renormalization procedure, potential, and overall options.

**Options dialog box:**

- Options for renormalization procedure: vlowk
- Options for Potential: CD-bonn
  - CIB
  - CSB
- Overall options:
  - Oscillator Energy (MeV): 14.0
  - Minimum J: 0
  - Maximum J: 6
  - Include Coulomb interaction

**Neutron orbits (Green particles):**

Orbit	Energy	Particles
1h 9/2	92	0
3s 1/2	82	0
2d 3/2	70	0
2d 5/2	68	0
1s 7/2	64	0
1s 5/2	58	0
1g 9/2	50	0
2p 1/2	40	0
2p 3/2	38	0
1f 7/2	32	0
1d 3/2	28	0
2s 1/2	20	0
1d 5/2	16	0
1d 3/2	14	0
1p 1/2	8	0
1p 3/2	6	0
1s 1/2	2	0

**Proton orbits (Red particles):**

Orbit	Energy	Particles
1h 9/2	92	0
3s 1/2	82	0
2d 3/2	70	0
2d 5/2	68	0
1s 7/2	64	0
1s 5/2	58	0
1g 9/2	50	0
2p 1/2	40	0
2p 3/2	38	0
1f 7/2	32	0
1d 3/2	28	0
2s 1/2	20	0
1d 5/2	16	0
1d 3/2	14	0
1p 1/2	8	0
1p 3/2	6	0
1s 1/2	2	0

# Numerical Solution, Simplifications

For scattering states, the energy is positive,  $E > 0$ . The Lippman-Schwinger equation, which is the non-relativistic version of the Bethe-Salpeter equation discussed above, is an integral equation where we have to deal with the amplitude  $R(k, k')$  (reaction matrix, which is the real part of the full complex  $T$ -matrix discussed in the previous section) defined through the integral equation

$$R_l(k, k') = V_l(k, k') + \frac{2}{\pi} \mathcal{P} \int_0^\infty dq q^2 V_l(k, q) \frac{1}{E - q^2/m} R_l(q, k').$$

The phaseshift codes are at

<http://www.fys.uio.no/compphys/cp/software.html>



# Numerical Solution, further Simplifications

The total kinetic energy of the two incoming particles in the center-of-mass system is

$$E = \frac{k_0^2}{m}.$$

The symbol  $\mathcal{P}$  indicates that Cauchy's principal-value prescription is used in order to avoid the singularity arising from the zero of the denominator.

The matrix  $R_l(k, k')$  relates to the the phase shifts through its diagonal elements as

$$R_l(k_0, k_0) = -\frac{\tan\delta_l}{mk_0}.$$

# Recipe I

From now on we will drop the subscript  $l$  in all equations. In order to solve the Lippman-Schwinger equation in momentum space, we need first to write a function which sets up the mesh points. We need to do that since we are going to approximate an integral through

$$\int_a^b f(x) dx \approx \sum_{i=1}^N w_i f(x_i),$$

where we have fixed  $N$  lattice points through the corresponding weights  $w_i$  and points  $x_i$ . Typically obtained via methods like Gaussian quadrature, see my course on computational physics (all material in english) <http://www.uio.no/studier/emner/matnat/fys/FYS3150/h08/>

## Recipe II

If you use Gauss-Legendre the points are determined for the interval  $x_i \in [-1, 1]$  You map these points over to the limits in your integral. You can then use the following mapping

$$k_i = \text{const} \times \tan \left\{ \frac{\pi}{4} (1 + x_i) \right\},$$

and

$$\omega_i = \text{const} \frac{\pi}{4} \frac{w_i}{\cos^2 \left( \frac{\pi}{4} (1 + x_i) \right)}.$$

If you choose units  $\text{fm}^{-1}$  for  $k$ , set  $\text{const} = 1$ . If you choose to work with MeV, set  $\text{const} \sim 200$  ( $\hbar c = 197 \text{ MeVfm}$ ).

## Recipe III

The principal value integral is rather tricky to evaluate numerically, mainly since computers have limited precision. We will here use a subtraction trick often used when dealing with singular integrals in numerical calculations. We introduce first the calculus relation

$$\int_{-\infty}^{\infty} \frac{dk}{k - k_0} = 0.$$

It means that the curve  $1/(k - k_0)$  has equal and opposite areas on both sides of the singular point  $k_0$ . If we break the integral into one over positive  $k$  and one over negative  $k$ , a change of variable  $k \rightarrow -k$  allows us to rewrite the last equation as

$$\int_0^{\infty} \frac{dk}{k^2 - k_0^2} = 0.$$

## Recipe IV

We can then express a principal values integral as

$$\mathcal{P} \int_0^{\infty} \frac{f(k)dk}{k^2 - k_0^2} = \int_0^{\infty} \frac{(f(k) - f(k_0))dk}{k^2 - k_0^2},$$

where the right-hand side is no longer singular at  $k = k_0$ , it is proportional to the derivative  $df/dk$ , and can be evaluated numerically as any other integral.

# Recipe V

We can then use this trick to obtain

$$R(k, k') = V(k, k') + \frac{2}{\pi} \int_0^\infty dq \frac{q^2 V(k, q) R(q, k') - k_0^2 V(k, k_0) R(k_0, k')}{(k_0^2 - q^2)/m}.$$

This is the equation to solve numerically in order to calculate the phase shifts. We are interested in obtaining  $R(k_0, k_0)$ .

## Recipe VI

How do we proceed?

Using the mesh points  $k_j$  and the weights  $\omega_j$ , we reach

$$R(k, k') = V(k, k') + \frac{2}{\pi} \sum_{j=1}^N \frac{\omega_j k_j^2 V(k, k_j) R(k_j, k')}{(k_0^2 - k_j^2)/m} - \frac{2}{\pi} k_0^2 V(k, k_0) R(k_0, k')$$

## Recipe VII

This equation contains now the unknowns  $R(k_i, k_j)$  (with dimension  $N \times N$ ) and  $R(k_0, k_0)$ .

We can turn it into an equation with dimension  $(N + 1) \times (N + 1)$  with a mesh which contains the original mesh points  $k_j$  for  $j = 1, N$  and the point which corresponds to the energy  $k_0$ .

Consider the latter as the 'observable' point. The mesh points become then  $k_j$  for  $j = 1, n$  and  $k_{N+1} = k_0$ .

With these new mesh points we define the matrix

$$A_{i,j} = \delta_{i,j} - V(k_i, k_j)u_j,$$



## Recipe VIII

where  $\delta$  is the Kronecker  $\delta$  and

$$u_j = \frac{2}{\pi} \frac{\omega_j k_j^2}{(k_0^2 - k_j^2)/m} \quad j = 1, N$$

and

$$u_{N+1} = -\frac{2}{\pi} \sum_{j=1}^N \frac{k_0^2 \omega_j}{(k_0^2 - k_j^2)/m}.$$

## Recipe IX

The first task is then to set up the matrix  $A$  for a given  $k_0$ . This is an  $(N+1) \times (N+1)$  matrix. It can be convenient to have an outer loop which runs over the chosen observable values for the energy  $k_0^2/m$ . *Note that all mesh points  $k_j$  for  $j = 1, N$  must be different from  $k_0$ . Note also that  $V(k_i, k_j)$  is an  $(N+1) \times (N+1)$  matrix.* With the matrix  $A$  we can rewrite the problem as a matrix problem of dimension  $(N+1) \times (N+1)$ . All matrices  $R$ ,  $A$  and  $V$  have this dimension and we get

$$A_{i,l} R_{l,j} = V_{i,j},$$

or just

$$AR = V.$$

# Recipe X

Since you already have defined  $A$  and  $V$  (these are stored as  $(N + 1) \times (N + 1)$  matrices) The final equation involves only the unknown  $R$ . We obtain it by matrix inversion, i.e.,

$$R = A^{-1}V.$$

Thus, to obtain  $R$ , you will need to set up the matrices  $A$  and  $V$  and invert the matrix  $A$ . With the inverse  $A^{-1}$ , perform a matrix multiplication with  $V$  results in  $R$ .

With  $R$  you can then evaluate the phase shifts by noting that

$$R(k_{N+1}, k_{N+1}) = R(k_0, k_0) = -\frac{\tan\delta}{mk_0},$$

where  $\delta$  are the phase shifts.

# Lippman-Schwinger Equation, Repeated

To parameterize the nucleon-nucleon interaction we solve the Lippman-Schwinger equation

$$T_{ll'}^\alpha(kk'K) = V_{ll'}^\alpha(kk') + \frac{2}{\pi} \sum_{l''} \int_0^\infty dq q^2 V_{ll''}^\alpha(kq) \frac{1}{k^2 - q^2 + i\epsilon} T_{l''l'}^\alpha(qk'K).$$

The shorthand notation

$$T(\hat{V})_{ll'}^\alpha(kk'K\omega) = \langle kKIL\mathcal{J}ST | T(\omega) | k'Kl'L\mathcal{J}ST \rangle,$$

denotes the  $T(V)$ -matrix with momenta  $k$  and  $k'$  and orbital momenta  $l$  and  $l'$  of the relative motion, and  $K$  is the corresponding momentum of the center-of-mass motion. Further,  $L$ ,  $\mathcal{J}$ ,  $S$  and  $T$  are the orbital momentum of the center-of-mass motion, the total angular momentum, spin and isospin, respectively.

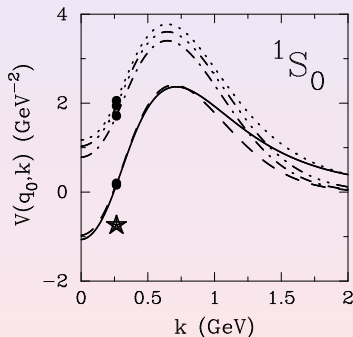
# Numerical Solution, Repeated

For scattering states, the energy is positive,  $E > 0$ . The Lippman-Schwinger equation, which is the non-relativistic version of the Bethe-Salpeter equation discussed above, is an integral equation where we have to deal with the amplitude  $R(k, k')$  (reaction matrix, which is the real part of the full complex  $T$ -matrix) defined through the integral equation for one partial wave (no coupled-channels)

$$R_l(k, k') = V_l(k, k') + \frac{2}{\pi} \mathcal{P} \int_0^\infty dq q^2 V_l(k, q) \frac{1}{E - q^2/m} R_l(q, k').$$

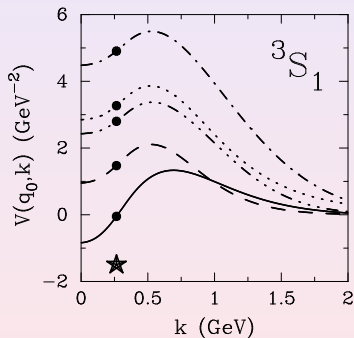
For negative energies (bound states) and intermediate states scattering states blocked by occupied states below the Fermi level, this expressions leads to the  $G$ -matrix to be discussed today.

# T-matrix and $V$

 $^1S_0$ 

Matrix elements  $V(q_0, k)$  for the  $^1S_0$  partial wave for the CD-Bonn (solid line), Nijm-I (dashed), Nijm-II (dash-dot), Argonne  $V_{18}$  (dash-triple-dot) and Reid93 (dotted) potentials. The diagonal matrix elements with  $k = q_0 = 265$  MeV/c (equivalent to  $T_{lab} = 150$  MeV) are marked by a solid dot. The corresponding matrix element of the full scattering  $R$ -matrix is marked by the star.

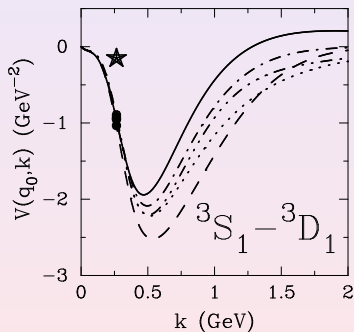
# T-matrix and V



## ${}^3S_1$

Matrix elements for the  ${}^3S_1$  for the CD-Bonn (solid line), Nijm-I (dashed), Nijm-II (dash-dot), Argonne  $V_{18}$  (dash-triple-dot) and Reid93 (dotted) potentials. The diagonal matrix elements with  $k = q_0 = 265 \text{ MeV}/c$  (equivalent to  $T_{lab} = 150 \text{ MeV}$ ) are marked by a solid dot. The corresponding matrix element of the full scattering  $R$ -matrix is marked by the star.

# T-matrix and V

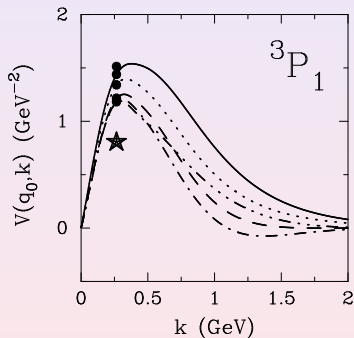


## ${}^3S_1-{}^3D_1$

Matrix elements for  ${}^3S_1-{}^3D_1$  for the CD-Bonn (solid line), Nijm-I (dashed), Nijm-II (dash-dot), Argonne  $V_{18}$  (dash-triple-dot) and Reid93 (dotted) potentials. The diagonal matrix elements with  $k = q_0 = 265$  MeV/c (equivalent to  $T_{lab} = 150$  MeV) are marked by a solid dot. The corresponding matrix element of the full scattering  $R$ -matrix is marked by the star.



# T-matrix and $V$



## ${}^3P_1$

Matrix elements for  ${}^3P_1$  for the CD-Bonn (solid line), Nijm-I (dashed), Nijm-II (dash-dot), Argonne  $V_{18}$  (dash-triple-dot) and Reid93 (dotted) potentials. The diagonal matrix elements with  $k = q_0 = 265$  MeV/c (equivalent to  $T_{lab} = 150$  MeV) are marked by a solid dot. The corresponding matrix element of the full scattering  $R$ -matrix is marked by the star.

# Does it matter?

The behavior seen here has important consequences for renormalizations in nuclear medium.

All interactions yield the same on-shell  $T$ -matrix, although  $V$  and its off-shell character can be very different from interaction model to interaction model. The off-shell part is not constrained by data. Potentials with for example a weak tensor force (cancellation between the  $\pi$  and  $\rho$  meson contributions) can lead to important differences in for example nuclear binding energies.

# OBE vs Chiral Perturbation Theory

Historically, the experimental discovery of heavy mesons in the early 1960s gave momentum to the one-boson-exchange (OBE) model. Prior to that it was pion physics which dominated the picture. The weak point of this model, however, is the scalar-isoscalar “sigma” or “epsilon” boson, for which the empirical evidence remains controversial. Since this boson is associated with the correlated (or resonant) exchange of two pions, a vast theoretical effort that occupied more than a decade (1970-1980) was launched to derive the  $2\pi$ -exchange contribution of the nuclear force, which creates the intermediate range attraction.

The nuclear force problem appeared to be solved; however, with the discovery of quantum chromo-dynamics (QCD), all “meson theories” had to be relegated to models and the attempts to derive the nuclear force started all over again.

# OBE vs Chiral Perturbation Theory

The problem with a derivation from QCD is that this theory is non-perturbative in the low-energy regime characteristic of nuclear physics, which makes direct solutions impossible. Therefore, during the first round of new attempts, QCD-inspired quark models became popular. These models were able to reproduce qualitatively some of the gross features of the nuclear force. But were useless for nuclear structure. Also, on a critical note, it has been pointed out that these quark-based approaches were nothing but another set of models and, thus, did not represent any fundamental progress. Equally well, one may then stay with the simpler and much more quantitative meson models.

# Chiral Perturbation Theory

A major breakthrough occurred when the concept of an effective field theory (EFT) was introduced and applied to low-energy QCD. As outlined by Weinberg in 1979 one has to write down the most general Lagrangian consistent with the assumed symmetry principles, particularly the (broken) chiral symmetry of QCD. At low energy, the effective degrees of freedom are pions and nucleons rather than quarks and gluons; heavy mesons and nucleon resonances are “integrated out”. So, in a certain sense we are back to the 1950s, except that we are smarter by 40 years of experience: broken chiral symmetry is a crucial constraint that generates and controls the dynamics and establishes a clear connection with the underlying theory, QCD.

# Chiral Perturbation Theory

Chiral Perturbation Theory (CHPT) is the effective theory of QCD and, more generally, of the Standard Model, which was formulated by Weinberg and developed in to a systematic tool for analyzing low-energy QCD by Gasser and Leutwyler. Consider the QCD Lagrangian in the two-flavor case of the light up and down quarks

$$\mathcal{L}_{\text{QCD}} = \bar{q} (i\gamma_\mu D^\mu - \mathcal{M}) q - \frac{1}{4} G_{\mu\nu}^a G^{a\mu\nu},$$

where  $D_\mu = \partial_\mu - ig_s G_\mu^a T^a$  with  $T^a$ , (with  $a = 1 \dots 8$ ) are the  $\text{SU}(3)_{\text{color}}$  Gell-Mann matrices and  $q$  the quark fields. Further,  $G_{\mu\nu}^a$  are the gluon field strength tensors, and the quark mass matrix is given by  $\mathcal{M} = \text{diag}(m_u, m_d)$ .

# Chiral Perturbation Theory

The left- and right-handed quark fields are defined by  $q_{L,R} = 1/2(1 \pm \gamma_5)q$ . The chiral group  $G$  is a group of independent  $SU(2)_{\text{flavor}}$  transformations of the left- and right-handed quark fields,  $G = SU(2)_L \times SU(2)_R$ . Expressing the quark part in the QCD Lagrangian in terms of  $q_{L,R}$ , it is easy to see that the covariant derivative term is invariant with respect to global chiral rotations, while the quark mass term is not. The running quark masses at the renormalization scale  $\mu = 1$  GeV are  $m_u \sim 5$  MeV and  $m_d \sim 9$  MeV. Given the fact that the masses of the up and down quarks are much smaller than the typical hadron scale of the order of 1 GeV, chiral  $SU(2)_L \times SU(2)_R$  symmetry can be considered as a rather accurate symmetry of QCD.

# Chiral Perturbation Theory

There is a strong evidence on both experimental and theoretical sides that chiral symmetry of QCD is spontaneously broken down to its vector subgroup (isospin group in the two-flavor case). Perhaps, the most striking evidence of the spontaneous breaking of the axial generators is provided by the nonexistence of degenerate parity doublets in the hadron spectrum and the presence of the triplet of unnaturally light pseudoscalar mesons (pions). The latter are natural candidates for the corresponding Nambu–Goldstone bosons which acquire a small nonzero mass due to the explicit chiral symmetry breaking by the nonvanishing quark masses.



# Effective Field Theories and QCD

## Two worlds

- At high energies: weak, asymptotic freedom; perturbative QCD.
- At low energies (= nuclear physics): strong QCD, non-perturbative; a totally different world.

The fact that the scenario at low- energy is so different from high-energy suggests that the effective description of the low-energy scenario should also be very different from high.

# Effective Field Theories and QCD

QCD in the  $u/d$  sector has approximate chiral symmetry but this symmetry is broken in two ways:

- Explicitly broken, because the  $u$  and  $d$  quark masses are not exactly zero;
- Spontaneously broken

$$SU(2)_L \times SU(2)_R \approx SU(2)_V \times SU(2)_A \rightarrow SU(2)_V,$$

that is in the QCD ground state, axial symmetry is broken, while isospin symmetry is intact.

We obtain 3 Goldstone bosons: the pions!

# Chiral Perturbation Theory

The chiral effective Lagrangian is given by an infinite series of terms with increasing number of derivatives and/or nucleon fields, with the dependence of each term on the pion field prescribed by the rules of broken chiral symmetry. Applying this Lagrangian to  $NN$  scattering generates an unlimited number of Feynman diagrams, which may suggest again an untractable problem. However, Weinberg showed that a systematic expansion of the nuclear amplitude exists in terms of  $(Q/\Lambda_\chi)^\nu$ , where  $Q$  denotes a momentum or pion mass,  $\Lambda_\chi \approx 1$  GeV is the chiral symmetry breaking scale, and  $\nu \geq 0$ . For a given order  $\nu$ , the number of contributing terms is finite and calculable; these terms are uniquely defined and the prediction at each order is model-independent. By going to higher orders, the amplitude can be calculated to any desired accuracy. The scheme just outlined has become known as chiral perturbation theory ( $\chi$ PT).

# Effective Field Theories

Therefore, we want to describe the low-energy scenario of QCD by an Effective Field Theory (EFT). The steps to take:

- Write down the most general Lagrangian including all terms consistent with the assumed symmetries, particularly, spontaneously broken chiral symmetry.
- Calculate Feynman diagrams. Note: There will be infinitely many diagrams.
- Find a scheme for assessing the importance of the various diagrams, because we cannot calculate infinitely many diagrams.

# Chiral Perturbation Theory

The starting point for the derivation of the  $NN$  interaction is an effective chiral Lagrangian

$$\mathcal{L} = \mathcal{L}_{\pi N} + \mathcal{L}_{\pi\pi} + \mathcal{L}_{NN},$$

which is given by a series of terms of increasing chiral dimension,

$$\mathcal{L}_{\pi N} = \mathcal{L}_{\pi N}^{(1)} + \mathcal{L}_{\pi N}^{(2)} + \mathcal{L}_{\pi N}^{(3)} + \dots,$$

$$\mathcal{L}_{\pi\pi} = \mathcal{L}_{\pi\pi}^{(2)} + \dots,$$

$$\mathcal{L}_{NN} = \mathcal{L}_{NN}^{(0)} + \mathcal{L}_{NN}^{(2)} + \mathcal{L}_{NN}^{(4)} + \dots,$$

where the superscript refers to the number of derivatives or pion mass insertions (chiral dimension). Good review: Epelbaum, Prog. Part. Nucl. Phys. **57**, 654 (2006).

# Chiral Perturbation Theory

Common to apply the heavy baryon (HB) formulation of chiral perturbation theory in which the relativistic Lagrangian is subjected to an expansion in terms of powers of  $1/M_N$  (kind of a nonrelativistic expansion), the lowest order of which is

$$\begin{aligned}\widehat{\mathcal{L}}_{\pi N}^{(1)} &= \bar{N} \left( iD_0 - \frac{g_A}{2} \vec{\sigma} \cdot \vec{u} \right) N \\ &\approx \bar{N} \left[ i\partial_0 - \frac{1}{4f_\pi^2} \boldsymbol{\tau} \cdot (\boldsymbol{\pi} \times \partial_0 \boldsymbol{\pi}) - \frac{g_A}{2f_\pi} \boldsymbol{\tau} \cdot (\vec{\sigma} \cdot \vec{\nabla}) \boldsymbol{\pi} \right] N + \dots\end{aligned}$$

For the parameters that occur in the leading order Lagrangian, we apply  $M_N = 938.919$  MeV,  $m_\pi = 138.04$  MeV,  $f_\pi = 92.4$  MeV, and  $g_A = g_{\pi NN} f_\pi / M_N = 1.29$ , which is equivalent to  $g_{\pi NN}^2 / 4\pi = 13.67$ .

# NN Interaction

The chiral NN force has the general form

$$V_{2N} = V_{\pi} + V_{\text{cont}} ,$$

where  $V_{\text{cont}}$  denotes the short-range terms represented by  $NN$  contact interactions and  $V_{\pi}$  corresponds to the long-range part associated with the pion-exchange contributions. Both  $V_{\pi}$  and  $V_{\text{cont}}$  are determined within the low-momentum expansion.

Notice that the nucleon kinetic energy contributes to  $\mathcal{L}^{(2)}$ . The above terms determine the nuclear potential up to N<sup>2</sup>LO (with the exception of the NN contact terms at NLO) in the limit of exact isospin symmetry.

# NN Interaction

Consider now pion-exchange contributions to the potential

$$V_{\pi} = V_{1\pi} + V_{2\pi} + V_{3\pi} + \dots ,$$

where one-, two- and three-pion exchange (3PE) contributions  $V_{1\pi}$ ,  $V_{2\pi}$  and  $V_{3\pi}$  can be written in the low-momentum expansion as

$$\begin{aligned} V_{1\pi} &= V_{1\pi}^{(0)} + V_{1\pi}^{(2)} + V_{1\pi}^{(3)} + V_{1\pi}^{(4)} + \dots , \\ V_{2\pi} &= V_{2\pi}^{(2)} + V_{2\pi}^{(3)} + V_{2\pi}^{(4)} + \dots , \\ V_{3\pi} &= V_{3\pi}^{(4)} + \dots . \end{aligned}$$

Here, the superscripts denote the corresponding chiral order and the ellipses refer to  $(Q/\Lambda)^5$ - and higher order terms. Contributions due to the exchange of four- and more pions are further suppressed:  $n$ -pion exchange diagrams start to contribute at the order  $(Q/\Lambda)^{2n-2}$ . Notice further that in addition to isopin-invariant contributions there are isospin-breaking corrections.



# NN Interaction

The static 1PE potential at N<sup>3</sup>LO has the form

$$V_{1\pi}^{(0)} + V_{1\pi}^{(2)} + V_{1\pi}^{(3)} + V_{1\pi}^{(4)} = - \left( \frac{g_A}{2F_\pi} \right)^2 (1 + \delta)^2 \boldsymbol{\tau}_1 \cdot \boldsymbol{\tau}_2 \frac{\vec{\sigma}_1 \cdot \vec{q} \vec{\sigma}_2 \cdot \vec{q}}{\vec{q}^2 + M_\pi^2} .$$

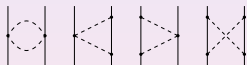
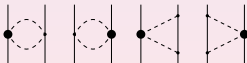
# NN Interaction

The 2PE contributions are convenient to express as  $V_{2\pi}$  in the form:

$$\begin{aligned} V_{2\pi} = & V_C + \boldsymbol{\tau}_1 \cdot \boldsymbol{\tau}_2 W_C + [V_S + \boldsymbol{\tau}_1 \cdot \boldsymbol{\tau}_2 W_S] \vec{\sigma}_1 \cdot \vec{\sigma}_2 + [V_T + \boldsymbol{\tau}_1 \cdot \boldsymbol{\tau}_2 W_T] \vec{\sigma}_1 \cdot \vec{q} \vec{\sigma}_2 \cdot \vec{q} \\ & + [V_{LS} + \boldsymbol{\tau}_1 \cdot \boldsymbol{\tau}_2 W_{LS}] i(\vec{\sigma}_1 + \vec{\sigma}_2) \cdot (\vec{q} \times \vec{k}) \\ & + [V_{\sigma L} + \boldsymbol{\tau}_1 \cdot \boldsymbol{\tau}_2 W_{\sigma L}] \vec{\sigma}_1 \cdot (\vec{q} \times \vec{k}) \vec{\sigma}_2 \cdot (\vec{q} \times \vec{k}), \end{aligned}$$

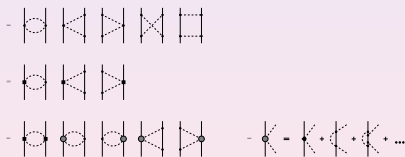
where the superscripts  $C$ ,  $S$ ,  $T$ ,  $LS$  and  $\sigma L$  of the scalar functions  $V_C, \dots, W_{\sigma L}$  refer to central, spin-spin, tensor, spin-orbit and quadratic spin-orbit components, respectively.

## Chiral Perturbation Theory

 $Q^0$ 1  $\pi$  Exchange $Q^2$ 2  $\pi$  Exchange $Q^3$  $\chi$ PT

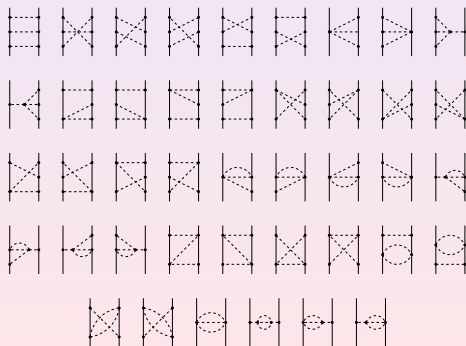
- The most important irreducible one- and two-pion exchange contributions to the  $NN$  interaction up to order  $Q^3$ .
- Vertices denoted by small dots are from  $\widehat{\mathcal{L}}_{\pi N}^{(1)}$ .
- Large dots refer to  $\widehat{\mathcal{L}}_{\pi N, ct}^{(2)}$

# $2\pi$ -Exchange

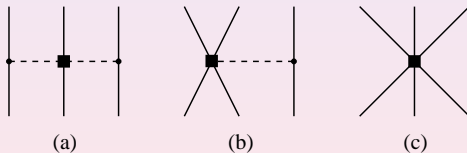


Leading  $((\frac{Q}{\Lambda})^2)$ , subleading  $((\frac{Q}{\Lambda})^3)$  and sub-subleading  $((\frac{Q}{\Lambda})^4)$  contributions to the chiral  $2\pi$ -exchange potential. Solid (dashed) lines correspond to nucleons (pions). Solid dots, filled rectangles and filled diamonds represent vertices with  $\Delta_i = 0, 1$  and  $2$ , respectively. Shaded blob denotes the next-to-next-to-leading order contribution to the pion-nucleon scattering amplitude.

# Leading contributions $3\pi$ -Exchange



# Three-Nucleon Force at order $\nu = 3$ .



# 3NF Interaction

The first non-vanishing 3NF contribution appears at order  $\nu = 3$ , i.e. at N<sup>2</sup>LO. The contribution from graph (a)

$$V_{2\pi}^{(3)} = \sum_{i \neq j \neq k} \frac{1}{2} \left( \frac{g_A}{2F_\pi} \right)^2 \frac{(\vec{\sigma}_i \cdot \vec{q}_i)(\vec{\sigma}_j \cdot \vec{q}_j)}{(\vec{q}_i^2 + M_\pi^2)(\vec{q}_j^2 + M_\pi^2)} F_{ijk}^{\alpha\beta} \tau_i^\alpha \tau_j^\beta,$$

where  $\vec{q}_i \equiv \vec{p}_i' - \vec{p}_i$ ;  $\vec{p}_i$  ( $\vec{p}_i'$ ) is the initial (final) momentum of the nucleon  $i$  and

$$F_{ijk}^{\alpha\beta} = \delta^{\alpha\beta} \left[ -\frac{4c_1 M_\pi^2}{F_\pi^2} + \frac{2c_3}{F_\pi^2} \vec{q}_i \cdot \vec{q}_j \right] + \sum_\gamma \frac{c_4}{F_\pi^2} \epsilon^{\alpha\beta\gamma} \tau_k^\gamma \vec{\sigma}_k \cdot [\vec{q}_i \times \vec{q}_j].$$

# 3NF Interaction

The contributions from the remaining graphs (b) and (c) take the form

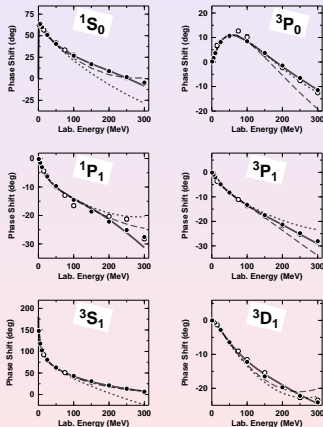
$$V_{1\pi, \text{cont}}^{(3)} = - \sum_{i \neq j \neq k} \frac{g_A}{8F_\pi^2} D \frac{\vec{\sigma}_j \cdot \vec{q}_j}{\vec{q}_j^2 + M_\pi^2} (\boldsymbol{\tau}_i \cdot \boldsymbol{\tau}_j) (\vec{\sigma}_i \cdot \vec{q}_j), \quad V_{\text{cont}}^{(3)} = \frac{1}{2} \sum_{j \neq k} E (\boldsymbol{\tau}_j \cdot \boldsymbol{\tau}_k),$$

where  $D$  and  $E$  are the corresponding low-energy constants from the Lagrangian of order  $\nu = 1$ .



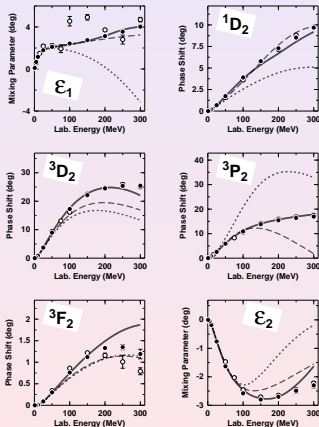
# NN and 3NF Interaction

Chiral order	2N force	3N force	4N force
$\nu = 0$	$V_{1\pi} + V_{\text{cont}}$	—	—
$\nu = 1$	—	—	—
$\nu = 2$	$V_{1\pi} + V_{2\pi} + V_{\text{cont}}$	—	—
$\nu = 3$	$V_{1\pi} + V_{2\pi}$	$V_{2\pi} + V_{1\pi, \text{cont}} + V_{\text{cont}}$	—
$\nu = 4$	$V_{1\pi} + V_{2\pi} + V_{3\pi} + V_{\text{cont}}$	work in progress	work in progress

Results with NN interaction to  $\nu = 4$ 

## Phase Shifts

- $np$  phase parameters below 300 MeV lab. energy for partial waves with  $J \leq 2$ . The solid line is the result at N<sup>3</sup>LO.
- The dotted and dashed lines are the phase shifts at NLO and NNLO, respectively.
- The solid dots show the Nijmegen multi-energy  $np$  phase shift analysis

Results with NN interaction to  $\nu = 4$ 

## Phase Shifts

- $np$  phase parameters below 300 MeV lab. energy for partial waves with  $J \leq 2$ . The solid line is the result at N<sup>3</sup>LO.
- The dotted and dashed lines are the phase shifts at NLO and NNLO, respectively.
- The solid dots show the Nijmegen multi-energy  $np$  phase shift analysis